

Synthesis, characterisation and biological activity of diorganotin compounds of (*E*)-*N'*-(5-nitro-2-hydroxybenzylidene)-3-hydroxy-2-naphthohydrazide[#]

**See Mun Lee^{a*}, Kong Mun Lo^a, Li Yuan Liew^b, Jactty Chew^b, Chun Hoe Tan^c,
Kae Shin Sim^c, Edward R. T. Tiekink^a**

^aResearch Centre for Crystalline Materials, School of Medical and Life Sciences,
Sunway University, 47500 Bandar Sunway, Selangor Darul Ehsan, Malaysia

^bDepartment of Biological Science, School of Medical and Life Sciences, Sunway
University, 47500 Bandar Sunway, Selangor Darul Ehsan, Malaysia

^cInstitute of Biological Sciences, Faculty of Science, Universiti Malaya,
50603 Kuala Lumpur, Malaysia

**Corresponding author: annielee@sunway.edu.my (S. M. Lee)*

[#] Dedicated to Prof. Dr Ionel Haiduc in recognition of a gentleman scholar

Diorganotin(IV) compounds with the general formula R_2SnL [$H_2L = (E)-N'$ -[1-(5-nitro-2-hydroxybenzylidene)-3-hydroxy-2-naphthohydrazide; $R = Me$ (**1**.toluene and **1**), $n-Bu$ (**2**), Ph (**3**), Cy (**4**), Bz (**5**), $o-ClBz$ (**6**) and $p-ClBz$ (**7**)] have been synthesised and characterised by elemental analyses, IR, 1H , $^{13}C\{^1H\}$ and ^{119}Sn NMR spectroscopy, thermal analysis and in the cases of **1** and **3**, single crystal X-ray diffraction. Crystallography, in accord with NMR, indicate highly distorted penta-coordinate geometries whereby each C_2NO_2 donor set is defined by the NO_2 donor atoms derived from di-anionic L and two tin-bound organo substituents. The

Schiff base ligand and the corresponding diorganotin compounds have been evaluated against two colon human carcinoma cell lines (HT-29 and HCT 116) and a normal colon fibroblast cell line (CCD-18Co). Among the evaluated compounds, the n-butyl derivative, **2**, is most potent and least toxic to the cancer and normal cell lines, respectively, yielding the highest safety profile (high SI). In addition, the anti-bacterial activities have been evaluated against a panel of 21 Gram positive and Gram negative bacteria. Based on the broth dilution method, non-toxic **3**, exhibited promising anti-bacterial effects against two Gram positive bacteria, namely, *Enterococcus faecalis* and *Staphylococcus epidermidis*.

Keywords: diorganotin, penta-coordination, X-ray structure, cytotoxic activity, anti-bacterial activity

1. Introduction

Organotin compounds have been widely studied owing to their well-documented versatile chemistry and their potential as biologically active compounds [1-9]. An important class of organotin compounds are those derived from Schiff bases. These have received great attention owing to their structural diversity, thermal stability and wide range of possible biological applications [10-12]. Organotin compounds of Schiff bases have been proposed to possess mild to good anti-cancer [12-17], anti-microbial [11, 14, 18-22], anti-leishmanial [23, 24] and anti-inflammatory [20, 25, 26] potentials.

The coordination chemistry of organotins is diverse, exhibiting various geometries and coordination numbers that vary from four to seven [27, 28]. This variety and adaptability prove to be a hindrance in rationalising the mode(s) of action behind the demonstrated biological activity of organotins. Qualitatively, the structure of organotin compounds, coordination number, the nature of the organic groups attached to the tin atom and the extent of the

alkylation/arylation could be prominent factors determining biological activity. Any modification in any one or more of the aforementioned factors could dramatically influence the observed biological activity. As a result, there is considerable interest in organotin Schiff base derivatives, especially those with various combinations of *N*-, *O*- and *S*- donor ligands [29-34]. This interest arises because Schiff bases can provide stable geometries due to the tridentate coordination mode of the ligands whereby they are able to restrict the flexibility of the adopted molecular structures.

Schiff bases derived from 3-hydroxy-2-naphthoylhydrazide are reported to have good anti-microbial activities [35]. Herein, as part of on-going work on organotin compounds with *ONO*-tridentate ligands [36-38], is reported the synthesis and structural studies (spectral and crystallographic) of new diorganotin Schiff base compounds where the Schiff base is derived from the condensation reaction of 3-hydroxy-2-naphthol-hydrazide with 5-nitrosalicylaldehyde. Moreover, the anti-bacterial activities, against a range of seven Gram positive and 14 Gram negative bacteria, as well as *in vitro* cytotoxicity profiles, against two colon human carcinoma cell lines, namely HT-29 and HCT 116, are described.

2. Experimental section

2.1 Physical measurements

The melting points of the ligand and diorganotin compounds were determined using an Electrothermal digital melting point apparatus and were uncorrected. Elemental analyses were carried out on a Perkin Elmer EA2400 CHNS Elemental Analyzer. The IR spectra for the compounds were recorded in KBr pellets on a Perkin-Elmer Spectrum RX1 FT-IR spectrophotometer. The ^1H and $^{13}\text{C}\{^1\text{H}\}$ NMR spectra were recorded on a JEOL JNM GX-270 FT NMR SYSTEM spectrometer while the ^{119}Sn NMR spectra were recorded on a JEOL ECA-400MHz spectrometer. The chemical shifts were recorded in ppm with reference to

Me₄Si for ¹H and ¹³C{¹H} NMR, and Me₄Sn for ¹¹⁹Sn NMR. Thermogravimetric analyses were performed on a Perkin Elmer TGA 4000 Thermogravimetric Analyzer in the range of 35–900 °C at a rate of 10°C/min.

2.2 Materials

All chemicals and reagents used in the synthesis were of reagent grade. Dimethyltin oxide (Acros), dibutyltin dichloride (Fluka), diphenyltin oxide (Acros), dicyclohexyltin oxide (Acros), 3-hydroxy-2-naphthoylhydrazide (Aldrich) and 5-nitrosalicylaldehyde (Fluka) were commercially available. Dibenzyltin dichloride, di(*o*-chlorobenzyl)tin dichloride and di(*p*-chlorobenzyl)tin dichloride were prepared in accordance with the literature method [39]. The solvents used in the reaction were of AR grade and dried using standard literature procedures [40].

The human-derived colorectal adenocarcinoma HT-29 (ATCC® HTB-38™), colorectal carcinoma HCT 116 (ATCC® CCL-247™) and normal colon fibroblast CCD-18Co (ATCC® CRL-1459™) were purchased from the American Type Culture Collection (ATCC, USA). Cells were cultured using McCoy's 5A Medium (HT-29 and HCT 116) or Eagle's minimum essential medium (CCD-18Co), supplemented with 10% fetal bovine serum, and incubated at 37 °C in a CO₂ incubator. Cells were sub-cultured upon reaching 70–80% confluency and maintained at a low-passage number with their morphology observed regularly.

A total of 21 bacterial species were used in this study; seven of which were Gram positive bacteria: *Bacillus cereus* (ATCC 10876), *Bacillus subtilis* (ATCC 6633), *Enterococcus faecalis* (ATCC 33186), *Enterococcus faecium* (ATCC 19434), methicillin-resistant *Staphylococcus aureus* (MRSA; MTCC 381123), *Staphylococcus epidermidis* (ATCC 700576) and *Staphylococcus saprophyticus* (ATCC 15305). The remaining 14 bacteria are Gram negative bacteria: *Acinetobacter baumannii* (ATCC 19117), *Aeromonas hydrophila*

(ATCC 35654), *Citrobacter freundii* (ATCC 8090), *Enterobacter aerogenes* (ATCC 13048), *Enterobacter cloacae* (ATCC 35030), *Escherichia coli* (ATCC 11775), *Escherichia coli* clinical isolate K1 (MTCC 710859), *Klebsiella pneumoniae* (ATCC 13883), *Klebsiella quasipneumoniae* (ATCC 49399), *Pseudomonas aeruginosa* (ATCC 10145), *Proteus vulgaris* (ATCC 49990), *Salmonella enterica* (ATCC 14028), *Shigella flexneri* (ATCC 12022) and *Stenotrophomonas maltophilia* (ATCC 13637). The bacterial cultures were maintained on Mueller Hinton Agar (MHA, Oxoid) and sub-cultured on a weekly basis. Prior to all experiments, the bacteria were cultured in Mueller-Hinton Broth (MHB, Oxoid) and incubated at 37 °C for 18 h to achieve log-phase.

2.3 Synthesis

2.3.1 Synthesis of (E)-N'-(5-Nitro-2-hydroxybenzylidene)-3-hydroxy-2-naphthohydrazide (H₂L)

3-Hydroxy-2-naphthoylhydrazide (2.02 g, 0.01 mol) and 5-nitrosalicylaldehyde (1.67 g, 0.01 mol) were dissolved in methanol (180 cm³) and refluxed for 2 h. Upon cooling to room temperature, a yellow solid was obtained and used without further purification.

Yield: 2.14 g, 61%; m.p. 324-326 °C. Anal. Calc. for C₁₈H₁₃N₃O₅: C, 61.54; H, 3.73; N, 11.96%. Found: C, 61.95; H, 3.56; N, 11.57%. IR (cm⁻¹): 3233 ν(O-H, N-H), 1638 ν(C=O), 1625 ν(C=N), 1075 ν(C-O).

2.3.2 Synthesis of diorganotin Schiff base compounds, 1-7

Compounds **3** and **4** were prepared according to the preparative method employed for **1** using the appropriate diorganotin oxide. The preparation method used for compound **2** was repeated for compounds **5**, **6** and **7** with the appropriate diorganotin chloride precursor.

2.3.2.1 [*N'*-(5-Nitro-2-oxidobenzylidene)-3-hydroxy-2-naphthohydrazidato]dimethyltin(IV),
*Me*₂*SnL*, **1**

H₂**L** (0.35 g, 1.0 mmol) in dry toluene (20 cm³) was added to a suspension of dimethyltin oxide (0.17 g, 1.0 mmol) in dry toluene (30 cm³). The mixture was heated under reflux in a Dean-Stark apparatus for 5 h to remove water formed during the reaction. The solvent was gradually removed by evaporation under vacuum until a yellow precipitate was obtained. The precipitate was recrystallised from toluene and the bulk compound was obtained as **1**.toluene (observed in ¹H and ¹³C{¹H} NMR spectra). A small amount of the precipitate was further recrystallised in a 1:1 mixture of dichloromethane-toluene to yield unsolvated yellow crystals suitable for X-ray crystallographic studies.

Yield: 0.39 g, 78%; m.p. 275-276 °C (single crystal sample). Anal. Calc. for C₂₀H₁₇N₃O₅Sn.C₇H₈: C, 54.96; H, 4.24; N, 7.12%. Found: C, 55.12; H, 3.79; N, 6.87%. IR (cm⁻¹): 3409 ν(O-H), 1639 ν(C=N), 1608 ν(C=N-N=C), 1174 ν(C-O), 703 ν(Sn-O), 466 ν(Sn-N).

2.3.2.2 [(5-Nitro-2-oxidobenzylidene)-3-hydroxy-2-naphthohydrazidato]dibutyltin(IV),
*Bu*₂*SnL*, **2**

H₂**L** (0.35 g, 1.0 mmol) and triethylamine (0.14 mL, 1.0 mmol) were added into absolute ethanol (30 cm³) and the mixture was heated under reflux for 2 h. Dibutyltin dichloride (0.30 g, 1.0 mmol) in absolute ethanol (20 cm³) was added and the mixture was refluxed for 5 h and filtered. The filtrate was concentrated to dryness under reduced pressure until a yellow precipitate was obtained. The precipitate was recrystallised from toluene and the by-product, triethylammonium chloride, was removed through filtration.

Yield: 0.50 g, 74%; m.p. 156-157 °C. Anal. Calc. for C₂₆H₂₉N₃O₅Sn: C, 53.64; H, 5.02; N, 7.21%. Found: C, 53.87; H, 4.94; N, 7.24%. IR (cm⁻¹): 3394 ν(O-H), 1639 ν(C=N), 1607 ν(C=N-N=C), 1170 ν(C-O), 704 ν(Sn-O), 463 ν(Sn-N).

2.3.2.3 [(5-Nitro-2-oxidobenzylidene)-3-hydroxy-2-naphthohydrazidato]diphenyltin(IV), Ph₂SnL, **3**

The precipitate of **3** was recrystallised from a 1:1 mixture of ethanol-toluene to yield yellow crystals suitable for X-ray crystallographic studies. Yield: 0.49 g, 75%; m.p. >350 °C. Anal. Calc. for C₃₀H₂₁N₃O₅Sn: C, 57.91; H, 3.37; N, 6.75%. Found: C, 57.55; H, 3.47; N, 6.69%. IR (cm⁻¹): 3411 ν(O-H), 1638 ν(C=N), 1610 ν(C=N-N=C), 1171 ν(C-O), 699 ν(Sn-O), 471 ν(Sn-N).

2.3.2.4 [(5-Nitro-2-oxidobenzylidene)-3-hydroxy-2-naphthohydrazidato]dicyclohexyltin(IV), Cy₂SnL, **4**

Yield: 0.48 g, 75%; m.p. 207-208 °C. Anal. Calc. for C₃₀H₃₃N₃O₅Sn: C, 56.83; H, 5.20; N, 6.62%. Found: C, 57.16; H, 5.77; N, 6.67%. IR (cm⁻¹): 3424 ν(O-H), 1639 ν(C=N), 1607 ν(C=N-N=C), 1170 ν(C-O), 704 ν(Sn-O), 475 ν(Sn-N).

2.3.2.5 [(5-Nitro-2-oxidobenzylidene)-3-hydroxy-2-naphthohydrazidato]dibenzyltin(IV), Bz₂SnL, **5**

Yield: 0.47 g, 73%; m.p. > 350 °C. Anal. Calc. for C₃₂H₂₅N₃O₅Sn: C, 59.12; H, 3.85; N, 6.46%. Found: C, 59.22; H, 3.63; N, 6.52%. IR (cm⁻¹): 3449 ν(O-H), 1638 ν(C=N), 1609 ν(C=N-N=C), 1170 ν(C-O), 699 ν(Sn-O), 476 ν(Sn-N).

2.3.2.6 [(5-Nitro-2-oxidobenzylidene)-3-hydroxy-2-naphthohydrazidato]di(*o*-chlorobenzyl)-tin(IV), (*o*-ClBz)₂SnL, **6**

Yield: 0.55 g, 77%; m.p. 202-204 °C. Anal. Calc. for C₃₂H₂₃Cl₂N₃O₅Sn: C, 53.44; H, 3.20; N, 5.84%. Found: C, 53.79; H, 3.32; N, 5.51%. IR (cm⁻¹): 3424 ν(O–H), 1639 ν(C=N), 1607 ν(C=N–N=C), 1172 ν(C–O), 705 ν(Sn–O), 478 ν(Sn–N).

2.3.2.7 [(5-Nitro-2-oxidobenzylidene)-3-hydroxy-2-naphthohydrazidato]di(*p*-chlorobenzyl)-tin(IV), (*p*-ClBz)₂SnL, **7**

Yield: 0.56 g, 78%; m.p. 218-220 °C. Anal. Calc. for C₃₂H₂₃N₃O₅Cl₂Sn: C, 53.44; H, 3.20; N, 5.84%. Found: C, 53.84; H, 3.23; N, 6.14%. IR (cm⁻¹): 3449 ν(O–H), 1639 ν(C=N), 1608 ν(C=N–N=C), 1171 ν(C–O), 706 ν(Sn–O), 477 ν(Sn–N).

2.4 X-ray structure determination

The intensity measurements on a yellow crystal of **1** (0.15 × 0.20 × 0.28 mm) were performed on an Agilent Technologies SuperNova Dual diffractometer [41] while those for yellow **3** (0.15 × 0.20 × 0.28 mm) were performed on a Rigaku Oxford Diffraction XtaLAB Synergy, Dualflex diffractometer [42]. Data were measured at 293 and 100 K, respectively, employing MoKα (λ = 0.71073 Å) and CuKα (λ = 1.54184 Å) radiation, respectively. The structures were solved by direct methods [43] and refined by a full-matrix least-squares procedure based on F^2 using SHELXL-2018/3 [44]. Then non-hydrogen atoms were refined with anisotropic displacement parameters, and the positions of carbon-bound hydrogen atoms were included in their calculated positions. The hydroxyl-H atoms were located in difference Fourier maps and were refined with O–H = 0.82±0.01 and 0.84±0.01 Å, respectively. A weighting scheme of the form $w = 1/[\sigma^2(F_o^2) + (aP)^2 + bP]$ where $P = (F_o^2 + 2F_c^2)/3$ was introduced towards the end of the refinement in each case. For **1**, owing to poor agreement,

one reflection, i.e. (-4 -1 1), was removed from the final cycles of refinement. The maximum and minimum residual electron density peaks noted at the conclusion of the refinement of **1**, i.e. 1.02 and -0.98 eÅ⁻³ were located 1.05 and 0.66 Å from the Sn atom, respectively. The molecular structure diagrams were generated with ORTEP for Windows [45] with 50% displacement ellipsoids, and the packing diagrams were drawn with DIAMOND [46]. Additional data analysis was made with PLATON [47]. **Crystallographic and refinement details are given in Table 1.**

Table 1

Crystallographic and refinement details for **1** and **3**.

Molecule	1	3
Formula	C ₂₀ H ₁₇ N ₃ O ₅ Sn	C ₃₀ H ₂₁ N ₃ O ₅ Sn
Molecular weight	498.05	622.19
Crystal system	triclinic	monoclinic
Space group	<i>P</i> $\bar{1}$	<i>C</i> 2/ <i>c</i>
<i>a</i> /Å	7.1488(3)	20.6084(1)
<i>b</i> /Å	11.6527(5)	17.2929(1)
<i>c</i> /Å	11.8130(4)	15.3233(1)
<i>α</i> /°	90.977(3)	90
<i>β</i> /°	100.426(3)	111.586(1)
<i>γ</i> /°	99.549(4)	90
<i>V</i> /Å ³	953.27(7)	5077.91(6)
<i>Z</i>	2	8
<i>D</i> _c /g cm ⁻³	1.735	1.628
<i>μ</i> /mm ⁻¹	1.379	8.405

Measured data	7501	30892
θ for 100% completeness /°	25.2	67.1
Unique data	4376	4539
R_{int}	0.051	0.026
Observed data ($I \geq 2.0\sigma(I)$)	3786	4469
No. parameters	267	355
R , obs. data	0.037	0.018
a and b in weighting scheme	0.021 and 0.218	0.028 and 4.518
$wR2$, all data	0.077	0.048
Range of residual electron density peaks/eÅ ⁻³	-0.98 – 1.02	-0.57 – 0.36

2.5 *In vitro* cytotoxic assay

The cytotoxicity of **H₂L** and **1–7** was evaluated by procedures described previously [48]. Briefly, 4×10^3 cells were seeded into a 96-well plate and incubated for 24 h, followed by treatment with various concentrations (0–100 μM) of the test compounds for 48 h, with cisplatin **being** the positive control. After the designated period of treatment, MTT (3-[4,5-dimethylthiazol-2-yl]-2,5-diphenyl-2H-tetrazolium bromide) was added to each well followed by incubation for a further 3 h before the addition of dimethylsulphoxide (DMSO). The absorbance of each well was then measured using a Tecan M200 Infinite Pro microplate reader at 570 nm, with 650 nm as the reference wavelength. The percentage of cell viability was calculated with reference to the untreated control, and the IC_{50} value was determined by plotting the percentage **viability** against the concentration of the test **compound** on a

logarithmic scale using the GraphPad Prism 7 software (Graphpad software Inc., CA, USA).

The selectivity index (SI) for the test compounds was calculated according to the equation:

$$SI = \frac{IC_{50} \text{ in CCD-18Co}}{IC_{50} \text{ in colorectal cancer cells (HT-29 or HCT 116)}}$$

where $SI > 2$ indicates the non-toxicity of a tested compound [49].

2.6 Anti-bacterial screening

2.6.1 Disc Diffusion assay

The anti-bacterial activity of the compounds was first screened using the disc diffusion method following the European Committee on Antimicrobial Susceptibility Testing (EUCAST) guidelines. The fresh overnight bacterial cultures were diluted to 0.5 McFarland turbidity standard, corresponding to approximately 10^8 colony forming units (CFU)/mL using phosphate buffer saline (PBS; Sigma-Aldrich). The adjusted inoculum suspension was then spread on MHA (Mueller Hinton Agar) sterile cotton swabs. Sterile filter paper discs (6 mm diameter) were aseptically placed on the agar. Each test compound (5 μ l) with a stock concentration of 6 mg/mL was added to the disc, resulting in a final concentration of 30 μ g/disc. Two discs loaded with known anti-biotics, tetracycline (30 μ g/disc) and chloramphenicol (30 μ g/disc), were included in the experiments as positive controls whereas discs containing DMSO (5 μ L) and broth medium (5 μ L) were included as solvent and negative controls, respectively. Plates with discs applied were incubated at 37 °C for 24 h. The anti-bacterial activities of the test compounds were determined by measuring the diameter of inhibition zones (in mm) formed around the discs. Three independent experiments were conducted for each compound tested for each bacterial species.

2.6.2 Determination of Minimum Inhibitory Concentration (MIC) and Minimum Bactericidal Concentration (MBC)

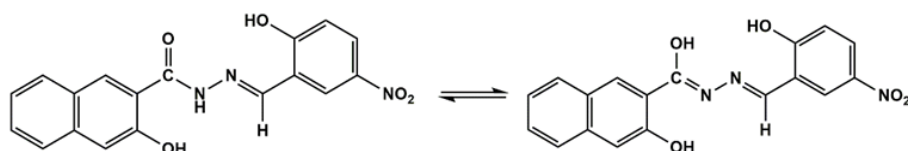
Following the disc diffusion screening, the determination of anti-bacterial activity of selected compounds which exhibited some preliminary activity was tested using the broth microdilution method in order to determine their MIC and MBC values. The broth-dilution method was conducted according to the Clinical & Laboratory Standards Institute (CLSI) protocol. Each test compound was prepared in DMSO to a concentration of 2 mg/mL, followed by a 2-fold titration using DMSO. Graded concentrations of test compounds (5 μ L each) were added into each well of 96-well microplates to achieve final concentrations ranging from 0.198 to 25 μ g/mL. Controls included in the assay were the anti-biotics (tetracycline and chloramphenicol, final concentrations ranging from 0.39 to 50 μ g/mL), DMSO (solvent) and medium (broth control). After the addition of the test compounds and controls, each inoculum suspension was added to wells, achieving 10^5 CFU/mL of cells in each well. Media with no bacterial suspension were also included as an additional negative control in the assay. The microplates were incubated for 24 h at 37 °C. The presence of turbidity observed in each well indicates the presence of bacterial growth. The MIC was determined as the lowest concentration at which no turbidity was seen. The suspension in each well was further separately aliquoted and transferred onto MHA. After a 24 h incubation at 37 °C, the MBC was determined as the minimal concentration of the test compound where no viable colony count was observed.

3. Results and discussion

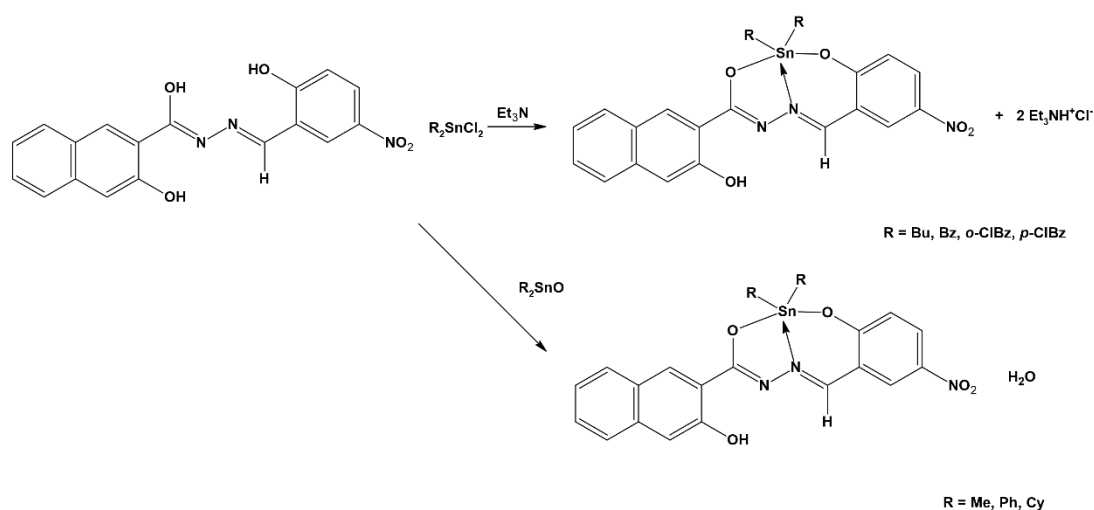
3.1 Synthesis

The Schiff base ligand, **H₂L**, was prepared from the stoichiometric reaction of 3-hydroxy-2-naphthoic hydrazide with 5-nitrosalicylaldehyde. **H₂L** may exist in two tautomeric forms as illustrated in Scheme 1, i.e. keto and enol forms, each capable of reacting readily with diorganotin oxides and diorganotin dichlorides, Scheme 2, to form **1-7**. Each of the prepared

organotin compounds, **1-7**, was obtained in good yield and was stable towards air and moisture. Compounds **1-4** were soluble in dichloromethane, chloroform and moderately soluble in polar solvents while compounds **5-7** were only moderately soluble in DMSO, dimethylformamide (DMF) and dioxane.



Scheme 1. Equilibrium between the keto-enol forms of **H₂L**.



Scheme 2. Reaction scheme for the synthesis of **H₂L** with diorganotin dichlorides and diorganotin oxides.

3.2 Spectroscopic data

3.2.1 FTIR spectroscopy

Selected infrared spectra data of **H₂L** and diorganotin compounds, **1-7**, are given in the Experimental section. A broad band at 3233 cm^{-1} in the IR spectrum of **H₂L** is attributed to the overlapping of $\nu(\text{N-H})$ and $\nu(\text{O-H})$. Upon complexation, a smaller band around $3300\text{-}3400\text{ cm}^{-1}$ is observed, suggesting the presence of a hydroxyl functional group in the molecular

structures of **1-7**. In addition, the IR spectrum of **H₂L** displays two sharp bands in the region 1620-1640 cm⁻¹ attributed to $\nu(\text{C}=\text{O})$ and $\nu(\text{C}=\text{N})$ stretching frequencies [50-52]. This shows that **H₂L** most likely exists in keto form in the solid-state. The lowering of the stretching frequencies of one of the bands is observed in the spectra of **1-7** whereby only one strong band is left from the initial two stretching bands. Meanwhile, another strong stretching band emerges around 1600 cm⁻¹ suggesting the involvement of the azomethine-N atom in coordination to the tin atom, thus weakening the C=N bond and leading to the formation of the $\nu(\text{C}=\text{N}-\text{N}=\text{C})$ fragment. The $\nu(\text{Sn}-\text{O})$ and $\nu(\text{Sn}-\text{N})$ bands are observed in the regions 690-710 and 460-480 cm⁻¹, respectively [53-55].

3.2.2 Multinuclear (¹H, ¹³C{¹H} and ¹¹⁹Sn) NMR

The ¹H, ¹³C{¹H} and ¹¹⁹Sn NMR data for **H₂L** and **1-7** are presented in Tables SI1, SI2, and Table 2, respectively; the ¹H and ¹³C{¹H} spectra are shown in Figs. SI1-SI16. Compound **1** was analysed as its 1:1 toluene solvate (Tables SI1 and SI2). Overall, all the compounds gave satisfactory spectra, exhibiting the expected resonances and integration (¹H). The resonance due to N-H in **H₂L** is absent in the spectra of **1-7**. While resonances (11.20-11.85 ppm) are still apparent for O-H in the spectra of **1-7**, which integrate for a single proton. These results confirm the double deprotonation of **H₂L** upon coordination to the respective diorganotin centres; X-ray crystallography (see below) confirms the hydroxyl group on the naphthalene ring does not participate in coordination to tin. A singlet around 8.60-8.74 is assigned to the proton of the azomethine carbon [36-38, 55-57].

The aromatic carbons of **H₂L** and **1-7** are found in the expected range, and their chemical shifts are in close agreement with reported values [56, 58]. The signal of the azomethine carbons (C-7) and (C-8) for **H₂L** appeared at 162.7 and 176.4 ppm, respectively

[57-59]. These resonances are shifted upfield, i.e. to 159.1-160.5 and 171.2-173.0 ppm, respectively, in **1-7**, supporting the formation of the Sn–N and Sn–O bonds.

For a number of the diorganotin compounds, satellite signals due to hydrogen-tin coupling and carbon-tin coupling were observed; the coupling constants are also reported in Tables SI1 and SI2. The geometry of the diorganotin compounds **in solution** can be predicted from the C–Sn–C angle **calculated using** the Lockhart and Manders' equation [60]:

$$\theta(\text{C–Sn–C}) = 0.0161|^2J(^{119}\text{Sn–}^1\text{H})|^2 - 1.32|^2J(^{119}\text{Sn–}^1\text{H})| + 133.4$$

The values of the two bond, $^2J(^{119}\text{Sn–}^1\text{H})$, coupling constants are in the range 72-82 Hz, indicative of penta-coordination. This conclusion is further corroborated by the $^{13}\text{C}\{^1\text{H}\}$ NMR data. **The C–Sn–C angles can be** estimated from the $^1J(^{119}\text{Sn–}^{13}\text{C})$ coupling constants using the **Lockhart** equation [61]:

$$\theta(\text{C–Sn–C}) = [|^1J(^{119}\text{Sn–}^{13}\text{C})| + 875]/11.4$$

The calculated C–Sn–C angles lie in the range 120-135°, which correspond to a distorted penta-coordinate environment around the central tin atom. A summary of the C–Sn–C angles calculated from the coupling constants is presented in **Table 2**.

Table 2

^{119}Sn NMR data for **1-7** and C–Sn–C angles estimated from coupling constants according to the Lockhart and Manders' and Lockhart's equations.

Comp'd	δ (ppm)	Lockhart and Manders' equation [60]	Lockhart's equation [61]
1^a	-156.5	125, 128	129, 130
2^a	-195.6	121, 125	124, 126
3^a	-355.5	n/a	119, 122
4^a	-263.4	122, 125	125, 127

5^b	-252.6	131, 133	128, 130
6^b	-270.5	128, 132	126, 128
7^b	-278.8	128, 131	127, 129

^a spectrum recorded in CDCl₃

^b spectrum recorded in 1,4-dioxane + 2-3 drops of CDCl₃

The ¹¹⁹Sn NMR spectra measured on **1-7** provide useful information regarding the coordination environment around the central tin atom. The presence of a single resonance in each ¹¹⁹Sn NMR spectrum confirms the formation of a single species; data are also included in **Table 2**. The ¹¹⁹Sn NMR chemical shifts fall into three distinct ranges depending on the nature of the tin-bound R group, i.e. **1** and **2**, **3** and **4-7** with the respective ranges consistent with a five-coordinate geometry for tin. In summary, the ¹¹⁹Sn NMR chemical shifts, ¹J(¹¹⁹Sn-¹H) and ¹J(¹¹⁹Sn-¹³C) coupling constants, when observed, support a penta-coordinate tin environment [62-65].

3.3 Thermal decomposition

Under thermogravimetric analysis (TG) conditions, diorganotin compounds **2-7** are stable until after 120 °C, and **exhibit** very similar decomposition profiles, **Table SI3**. Beyond 120 °C, the TG curves **2-7** exhibit three steps with weight loss. The first decomposition in the temperature range of 130-270 °C involves the loss of both alkyl or aryl groups. After this, a rapid weight loss is observed in the temperature range 240-410 °C **which corresponds** to the removal of the -NN-C(H)C₆H₅(O)NO₂ fragment. The final step was the gradual weight loss in the temperature range of 320-860 °C, equating to the loss of the -OCC₁₀H₆OH fragment. These results imply the weight **loss** in the second and third steps is due to the clean dissociation

of the Schiff base ligand from the tin centre [66, 67]. Overall, the thermal decomposition in the diorganotin compounds continues until the final residue, SnO, is left in the pan.

The exceptional decomposition pathway is evident for **1**.toluene where the first step sees loss of solvent in the range 80-130 °C. The remaining decomposition pathway mirrors those described for **2-7**, Table SI3; representative traces, i.e. for **1** and **7**, are shown in Figs. SI17 and SI18, respectively.

3.4 X-ray structure of **1** and **3**

The molecular structures of two representative molecules, namely **1** and **3**, were established by X-ray crystallography, as illustrated in Fig. 1, and selected geometric parameters listed in Table 3. In **1**, the tin atom is coordinated in an *ONO*-tridentate mode by the di-anionic Schiff base ligand. The C₂NO₂ donor set is completed by two methyl-C atoms. An indication of a five-coordinate coordination geometry is based on the value of τ , defined as $\tau = (\beta - \alpha)/60$, where α and β are the two widest donor-metal-donor angles. The value of τ computes to zero for a perfect square-pyramidal geometry and unity for a perfect trigonal-bipyramidal geometry [68]. In **1**, $\tau = 0.49$, i.e. almost exactly between the two ideal geometries. This is consistent with the significant deviation from linearity of the O1–Sn–O2 angle and the widening of the C21–Sn–C31 angle, Table 3.

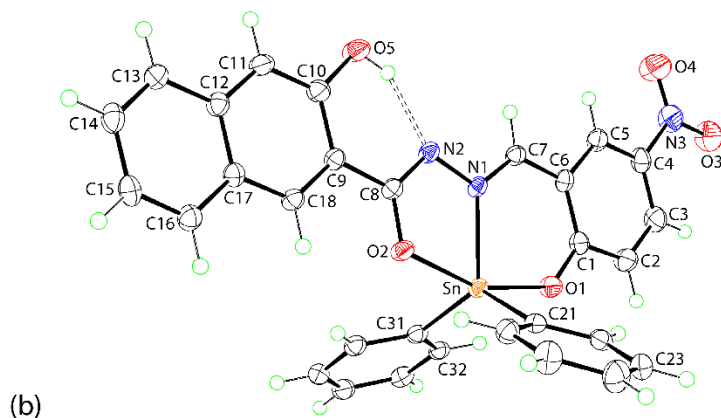
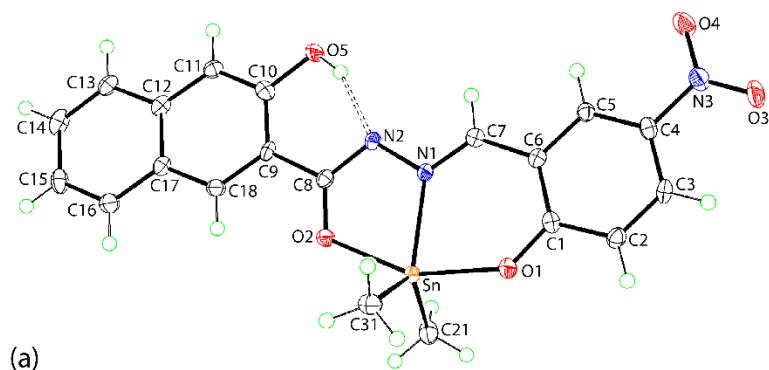


Fig. 1. The molecular structures of (a) **1** and (b) **3**, showing the atom-labelling schemes and 50% probability displacement ellipsoids.

Table 3

Selected geometric parameters (Å, °) for **1** and **3**.

Parameter	1	3
Sn–O1	2.101(2)	2.0749(12)
Sn–O2	2.143(2)	2.1237(11)
Sn–N1	2.200(3)	2.1743(13)
N1–N2	1.398(3)	1.3970(19)
C1–O1	1.313(4)	1.307(2)
C8–O2	1.289(4)	1.2983(19)

C7–N1	1.297(4)	1.296(2)
C8–N2	1.319(4)	1.320(2)
C6–C7	1.435(4)	1.446(2)
O1–Sn–O2	154.95(9)	158.02(5)
N1–Sn–C21	116.89(12)	116.70(5)
N1–Sn–C31	116.82(12)	112.18(5)
C21–Sn–C31	125.75(14)	130.88(6)

The tridentate mode of coordination of L^{2-} results in the formation of five- and six-membered chelate rings. The former is planar, exhibiting a r.m.s. = 0.0121 Å with the maximum deviation from the least-squares plane being 0.012(1) Å for the tin atom. Similarly, the larger chelate ring approximates a plane with a r.m.s. = 0.0254 Å but with a significantly greater maximum deviation of 0.0432(18) Å for the O1 atom. The dihedral angle between the chelate rings is 1.73(8)°. The approximate planarity in L^{2-} continues to the pendant organic residues with the dihedral angle between the five-membered chelate ring and the bound naphthyl residue being 6.91(8)°, and that between the fused six-membered rings being 1.94(9)°; the dihedral angle between the outer residues is 4.70(9)°. In terms of geometric parameters, the Sn–O1 bond length is a considerable 0.04 Å shorter than Sn–O2. This difference is reflected in the associated C–O bond lengths which is consistent with significant double bond character in the C8–O2 bond. This observation notwithstanding, delocalisation of π -electron density over the ligand backbone is indicated by systematic variations within this fragment, [Table 3](#), notably within the six-membered chelate ring. Finally, an intramolecular

hydroxy-O5-H \cdots N2(hydrazide) hydrogen bond is evident [O5 \cdots N2 = 2.601(3) Å; O5-H \cdots N2 = 156(3)°].

As might be anticipated, the molecular structure of **3** presents very similar features to those just described, [Table 3](#). The value of τ in this case computes to 0.45, suggestive of a small deviation towards a square-pyramidal geometry. The five- ([r.m.s.](#) = 0.0257 Å; maximum deviation = 0.0339(8) Å for atom O2) and six-membered ([r.m.s.](#) = 0.0222 Å; maximum deviation = 0.0316(9) Å for atom N1) chelate rings are approximately planar and form a dihedral angle = 3.11(5)°. The dihedral angles between the smaller and larger chelate rings and attached residues are 1.88(5) and 0.73(7)°, respectively, and the dihedral angle between the pendant groups is 5.54(7)°. As noted from [Table 3](#), the systematic variations in key geometric parameters persist with the only notable discrepancy seen in the disparity in the [N1-Sn-C21 and N1-Sn-C31 angles](#). The parameters associated with the intramolecular hydroxy-O5-H \cdots N2(hydrazide) hydrogen bond: O5 \cdots N2 = 2.650(2) Å; O5-H \cdots N2 = 151(2)°.

The crystallographic results mirror the spectroscopic conclusions. Further, the C21-Sn-C31 angles in **1** and **3** of 125.75(14) and 130.88(6)°, respectively, compare well with the data included in [Table 2](#) based on coupling constants, especially in consideration that the data refer to the solid- and solution-phases. Penta-coordinate geometries are indicated in each case and as the *ONO*-tridentate ligand is rigid in its mode of coordination, similar coordination geometries can be anticipated. This conclusion is further supported by a search of the Cambridge Structural Database [69]. There are eight closely related diorganotin structures containing the pendant naphthyl substituent, differing only in the nature of the substituents in the phenoxy ring. A summary of the structures obtained from this search as well values of τ are listed in [Table 4](#). Clearly, there is significant homogeneity in the penta-coordinate geometries regardless of the tin- and ligand-bound substituents and so it can be safely assumed

that the molecular structures of **2** and **4-7** are represented by the crystallographically determined structures of **1** and **3**.

Table 4

Summary of literature structures related to **1-7**.

R	Substituent in phenoxy ring	τ	Refcode	Ref.
Me (1)	5-NO ₂	0.49	–	this work
Me	5-Cl	0.47	FOVLAE	[70]
Me	5-Br	0.46	DULWOX	[71]
Me	4-O(CH ₂) ₉ CH ₃	0.52	ZARPOA	[72]
n-Bu	5-Cl	0.46	TECBUA	[37]
n-Bu	5-Br	0.43	POWSOK	[73]
Ph (3)	5-NO ₂	0.45	–	this work
Ph	5-Cl	0.53	RUPVII	[74]
Cy	5-Br	0.50	DULWUD	[75]
2-ClBz	5-Br	0.32	TECCAH	[37]

The molecular packing of **1** features naphthyl-C–H \cdots O(nitro), methyl-C–H \cdots O(hydroxyl), parallel nitro-O \cdots π (naphthyl) and π (nitrobenzene) \cdots π (naphthyl) interactions leading to a supramolecular layer in the *ac*-plane. Layers stack without directional interactions between **them**; see Figure SI19 for data and diagrams. In **3**, the three-dimensional architecture features naphthyl-C–H \cdots O(nitro), phenyl-C–H \cdots O(hydroxyl), nitrophenyl-C–H \cdots π (phenyl), phenyl-C–H \cdots π (phenyl) and parallel nitro-O \cdots π (naphthyl) interactions; details are given in Figure SI20.

3.5 Cytotoxic activity of **H₂L**, **1-7** and **S1-S7**

Cytotoxicity data are collated in **Table 5**. The ligand, **H₂L** demonstrated minimal cytotoxicity against human colorectal adenocarcinoma HT-29, with an IC₅₀ of 71.32 μM after 48 h of treatment. Upon complexation to form **1-7**, the cytotoxicity was notably enhanced with the most potent derivative being **7** (IC₅₀ 5.50 μM), for which IC₅₀ is ~13-fold more potent than **H₂L**. Similar to HT-29, **H₂L** exhibited lower cytotoxicity against human colorectal carcinoma HCT 116 (IC₅₀ 35.75 μM) than **1-7**, with **2** being particularly cytotoxic (IC₅₀ 1.44 μM). Moreover, nearly all compounds exhibited greater cytotoxicity than the commonly used chemotherapeutic drug, cisplatin, except for **3** (IC₅₀ 61.37 μM) in HT-29. Since the HCT 116 cell line has **a** wild-type tumour suppressor p53, and HT-29 is a p53-mutant [76], the observation that almost all test compounds exhibit greater cytotoxicity against the HCT 116 cell line suggests **their** anti-proliferative mechanisms could be facilitated by **functional** p53 in the cell. A definitive conclusion regarding the mechanisms can only be drawn when more assays are conducted, such as microarray and real time-PCR analyses.

A normal human colon fibroblast (CCD-18Co) was also included in the assay and all tested compounds are non-toxic (IC₅₀ > 100 μM) to the cells, except for **4** and **7**. The selectivity index (SI) was calculated to provide a preliminary insight into the safety of the tested compounds. Based on the values of SI, most tested compounds can be classified as highly selective (SI > 2), with the exception of **H₂L**, **3**, **4** and **S6** in HT-29.

Table 5Cytotoxic activity of H₂L and organotin compounds.^a

Compound	IC ₅₀ (μM)								
	HT-29			HCT 116			CCD-18Co		
	Mean	SD	SI	Mean	SD	SI	Mean	SD	
H ₂ L	71.32	4.07	1.40	35.75	2.75	2.80	> 100	-	
S1	> 100	-	-	> 100	-	-	> 100	-	
1	11.08	0.78	9.03	17.44	0.19	5.73	> 100	-	
S2	4.04	0.38	2.07	0.61	0.03	13.69	8.35	0.69	
2	13.54	0.85	7.39	1.44	0.06	69.44	> 100	-	
S3	7.36	0.66	3.80	2.32	0.08	12.05	27.95	1.63	
3	61.37	0.68	1.63	5.01	0.21	19.96	> 100	-	
S4	3.37	0.31	1.94	0.56	0.02	11.68	6.54	0.15	
4	14.14	0.64	1.90	2.18	0.14	12.35	26.93	2.52	
S5	8.07	0.47	2.80	4.87	0.42	4.64	22.6	0.89	
5	20.86	1.02	4.79	14.14	0.64	7.07	> 100	-	
S6	7.45	0.21	1.27	2.14	0.15	4.43	9.49	0.90	
6	34.57	2.76	2.89	7.66	0.62	13.05	> 100	-	
S7	5.47	0.33	1.95	3.12	0.14	3.42	10.68	0.95	
7	5.50	0.26	6.30	3.31	0.12	10.47	34.66	1.93	
Cisplatin	44.33	4.34	6.24	21.06	2.00	13.14	0.28 mM	0.02 mM	

^a S1 = dimethyltin oxide; S2 = di-n-butyltin dichloride; S3 = diphenyltin oxide; S4 = dicyclohexyltin oxide; S5 = dibenzyltin dichloride; S6 = di(*o*-chlorobenzyl)tin dichloride; S7 = di(*p*-chlorobenzyl)tin dichloride

As observed from Table 5, most of the organotin precursors, i.e. S1-S7, are far more potent than the Schiff base and 1-7; this has been commented upon previously [30]. This observation could be due to the greater molecular weight of 1-7 vs S1-S7. As the molecular weight and size of the molecules increase after complexation, 1-7 have a reduced tendency to permeate through the cellular membrane which has fixed pore size. Moreover, with the addition of L²⁻ into the precursors with loss of the non-organic ligands, the compounds tend to become less lipophilic, so the diffusion of the complexes across the hydrophobic cellular membranes could be hindered. This would result in reduced intracellular concentrations of 1-7 cf. S1-S7, hence leading to reduced cytotoxicity.

Overall, the complexation of H₂L to form 1-7 resulted in greater cytotoxicity and selectivity, indicating that complexation has substantially activated the cytotoxicity of H₂L. In particular, 2 can be considered as a candidate for further investigation for anti-cancer potential, as it exhibited the greatest cytotoxicity against both human colorectal cancer cell lines, greater activity than cisplatin, non-toxicity in normal human colon fibroblast and a high safety profile (high SI).

3.6 Anti-bacterial activity

3.6.1 Anti-bacterial screening of H₂L and 1-7

The anti-bacterial activity of H₂L and 1-7 was evaluated against 21 clinically important bacterial pathogens, including those listed on the WHO priority list of anti-biotic resistant bacteria, such as *Enterococcus faecium*, *Staphylococcus aureus* (Methicillin-resistant *Staphylococcus aureus*), *Acinetobacter baumannii*, *Klebsiella quasipneumoniae* and *Pseudomonas aeruginosa* [77]. New effective anti-bacterial agents are in urgent need for these pathogens.

Using the disc diffusion method, all organotin precursors, **S1-S7**, demonstrated anti-bacterial activity with the results compared with those obtained for the standard anti-biotics tetracycline and chloramphenicol, chosen owing to their having broad-spectrum anti-bacterial activity against both Gram positive and Gram negative bacteria (Table 6). Di-n-butyltin dichloride (**S2**) and diphenyltin dichloride (**S3**) showed comparable broad-spectrum anti-bacterial effects most of the Gram-positive and Gram-negative bacteria evaluated. In comparison, dimethyltin dichloride (**S1**) showed anti-bacterial activity against only selected Gram-positive and Gram-negative bacterial species. In contrast, dicyclohexyltin dichloride (**S4**) and the dibenzyltin derivatives (**S5**, **S6** and **S7**) exhibited anti-bacterial activity against only Gram-positive bacteria, with the exception of **S5** which showed marginal anti-bacterial effects on two Gram-negative bacteria: *Aeromonas hydrophila* and *Proteus vulgaris*. In contrast, zone inhibition and the resulting anti-bacterial activity of **1-7** were not observed when tested using the disc diffusion method.

Table SI4 summaries the cytotoxicity of **H₂L**, **S1-S7** and **1-7** towards the human embryonic kidney cell line (HEK293T). It is noteworthy that **1-7** were found to be generally less potent than their precursors, except for **1** and **S1** where the reverse is true. The anti-bacterial properties of two relatively less-cytotoxic compounds, i.e. **3** and **6**, were selected for further investigation using the broth dilution method (Table 7). The results suggest both **3** and **6** have limited anti-bacterial activity on Gram negative bacteria. However, **3** demonstrated potent anti-bacterial effect against two Gram positive bacteria, namely, *Enterococcus faecalis* and *Staphylococcus epidermidis*. Against these bacteria, the activity of **3** was comparable to that exhibited by chloramphenicol.

Table 6

Anti-bacterial activity of 1-7, precursors S1-S7 and H₂L screened using the disc diffusion method and interpreted by the zone of inhibition (mm).^a Standard anti-biotics, tetracycline (Tet) and chloramphenicol (Chlo), were also included in the study. Discs containing 30 µg of compound/standard/antibiotics were used.

Bacterial Species	1	S1	2	S2	3	S3	4	S4	5	S5	6	S6	7	S7	H ₂ L	Tet	Chlo
Gram-positive bacteria																	
<i>B. cereus</i>	-	11	-	14	-	15	-	10	-	10	-	8	-	7	-	20	27
<i>B. subtilis</i>	-	19	-	20	-	18	-	14	-	11	-	10	-	7	-	30	30
<i>E. faecalis</i>	-	-	-	16	-	16	-	12	-	12	-	10	-	8	-	32	30
<i>E. faecium</i>	-	-	-	12	-	14	-	12	-	10	-	8	-	8	-	27	26
<i>S. aureus</i> (MRSA)	-	-	-	15	-	18	-	10	-	10	-	10	-	8	-	26	24
<i>S. epidermidis</i>	-	16	8	21	-	20	-	14	-	11	-	11	-	8	-	32	32
<i>S. saprophyticus</i>	-	15	-	18	-	18	-	12	-	12	-	10	-	8	-	36	32
Gram-negative bacteria																	
<i>A. baumannii</i>	-	-	-	8	-	8	-	-	-	-	-	-	-	-	-	26	-
<i>A. hydrophila</i>	-	-	-	10	-	12	-	-	-	8	-	-	-	-	-	26	32
<i>C. freundii</i>	-	-	-	13	-	10	-	-	-	-	-	-	-	-	-	24	27
<i>E. aerogenes</i>	-	-	-	8	-	-	-	-	-	-	-	-	-	-	-	20	22
<i>E. cloacae</i>	-	-	-	8	-	-	-	-	-	-	-	-	-	-	-	20	26
<i>E. coli</i> ATCC 11775	-	10	-	9	-	8	-	-	-	-	-	-	-	-	-	22	25
<i>E. coli</i> K1	-	-	-	9	-	8	-	-	-	-	-	-	-	-	-	24	26
<i>K. pneumoniae</i>	-	12	-	16	-	12	-	-	-	-	-	-	-	-	-	26	32
<i>K. quasipneumoniae</i>	-	10	-	8	-	8	-	-	-	-	-	-	-	-	-	26	30
<i>P. aeruginosa</i>	-	12	-	-	-	-	-	-	-	-	-	-	-	-	-	-	-
<i>P. vulgaris</i>	-	-	-	12	-	9	-	-	-	8	-	-	-	-	-	13	21
<i>S. enterica</i>	-	-	-	10	-	8	-	-	-	-	-	-	-	-	-	21	24
<i>S. flexneri</i>	-	-	-	16	-	12	-	-	-	-	-	-	-	-	-	30	34
<i>S. maltophilia</i>	-	-	-	13	-	7	-	-	-	-	-	-	-	-	-	21	29

^a The smallest zone of inhibition (mm) is recorded in this Table as determined in three independent studies.

Table 7

MIC ($\mu\text{g/mL}$) and MBC ($\mu\text{g/mL}$) of **3**, **6**, tetracycline and chloramphenicol against 21 clinically important bacterial pathogens^{a, b, c}

Bacterial Species	3		6		tetracycline		chloramphenicol	
	MIC	MBC	MIC	MBC	MIC	MBC	MIC	MBC
Gram Positive								
<i>B. cereus</i>	12.5	>25	>25	> 25	3.125	12.5	3.125	> 50
<i>B. subtilis</i>	>25	>25	>25	>25	≤ 0.39	12.5	3.125	>50
<i>E. faecalis</i>	6.25	> 25	>25	>25	≤ 0.39	3.125	3.125	25
<i>E. faecium</i>	>25	>25	>25	>25	0.78	50	6.25	>50
<i>S. aureus</i> (MRSA)	> 25	>25	> 25	>25	≤ 0.39	12.5	12.5	50
<i>S. epidermidis</i>	3.125	>25	12.5	>25	≤ 0.39	≤ 0.39	3.125	6.25
<i>S. saprophyticus</i>	25	> 25	>25	> 25	≤ 0.39	1.56	6.25	25
Gram Negative								
<i>A. baumannii</i>	>25	>25	>25	>25	0.78	25	50	>50
<i>A. hydrophila</i>	>25	>25	>25	>25	≤ 0.39	25	0.78	>50
<i>C. freundii</i>	>25	>25	>25	>25	1.56	50	6.25	>50
<i>E. aerogenes</i>	>25	>25	>25	>25	1.56	>50	12.5	>50
<i>E. cloacae</i>	>25	>25	>25	>25	1.56	>50	6.25	>50
<i>E. coli</i> ATCC 11775	>25	>25	>25	>25	1.56	>50	6.25	>50
<i>E. coli</i> K1	>25	>25	>25	>25	0.78	>50	3.125	>50
<i>K. pneumoniae</i>	>25	>25	>25	>25	0.78	25	3.125	12.5
<i>K. quasipneumoniae</i>	>25	>25	>25	>25	1.56	>50	6.25	>50
<i>P. aeruginosa</i>	>25	>25	>25	>25	50	>50	>50	NA
<i>P. vulgaris</i>	>25	>25	>25	>25	25	>50	25	NA
<i>S. enterica</i>	>25	>25	>25	>25	0.78	>50	3.125	>50
<i>S. flexneri</i>	>25	>25	>25	>25	3.125	>50	1.56	25
<i>S. maltophilia</i>	>25	>25	>25	>25	1.56	>50	3.125	>50

^a MIC: minimum inhibitory concentration ($\mu\text{g/mL}$); MBC: minimum bactericidal concentration ($\mu\text{g/mL}$)

^b the presented MIC values are the lowest inhibitory concentrations obtained from three independent experiments conducted in triplicate

^c NA = not available

4. Conclusions

The diorganotin Schiff base compounds have distorted penta-coordinated geometries, as shown by the available X-ray structures and spectroscopic data. The cytotoxic activity of H₂L improved upon coordination, as its di-anion, to diorganotin. The di-n-butyltin derivative **2** emerges as a promising candidate for further anti-cancer investigations being non-toxic in normal human colon fibroblast cells, exhibiting the greatest potency against both human colorectal cancer cell lines studied, having a high safety profile (high SI) and being more potent compared with cisplatin. Finally, the anti-bacterial (broth dilution method) testing shows the diphenyltin species **3** demonstrated potential anti-bacterial effects against two Gram positive bacteria, namely, *E. faecalis* and *S. epidermidis*.

Declaration of Competing Interest

The authors declare that they have no known competing financial interests or personal relationships that could have appeared to influence the work reported in this paper.

Acknowledgements

The authors gratefully acknowledge Sunway University Sdn Bhd (Grants GRTIN-IRG-01-2021 and GRTIN-IRG-08-2021) for support of this research. The authors are also grateful to the University of Malaya for financial assistance (Grant: RP017B-14AFR) and the Ministry of Higher Education of Malaysia (MOHE) Fundamental Research Grant Scheme (FRGS; Grant: FP033-2014B) for supporting this research.

Abbreviations

A. baumannii

Acinetobacter baumannii

A. hydrophila

Aeromonas hydrophila

<i>B. cereus</i>	<i>Bacillus cereus</i> methicillin-resistant
<i>B. subtilis</i>	<i>Bacillus subtilis</i>
<i>C. freundii</i>	<i>Citrobacter freundii</i>
CCD-18Co	normal colon fibroblast
<i>E. aerogenes</i>	<i>Enterobacter aerogenes</i>
<i>E. cloacae</i>	<i>Enterobacter cloacae</i>
<i>E. coli</i>	<i>Escherichia coli</i>
<i>E. coli</i> K1	<i>Escherichia coli</i> clinical isolate K1
<i>E. faecalis</i>	<i>Enterococcus faecalis</i>
<i>E. faecium</i>	<i>Enterococcus faecium</i>
EUCAST	European Committee on Antimicrobial Susceptibility Testing
HT-29	human-derived colorectal adenocarcinoma
HCT116	colorectal carcinoma (ATCC® CCL-247™)
<i>K. pneumoniae</i>	<i>Klebsiella pneumoniae</i>
<i>K. quasipneumoniae</i>	<i>Klebsiella quasipneumoniae</i>
MBC	Minimum Bactericidal Concentration
MHA	Mueller Hinton Agar
MIC	Minimum Inhibitory Concentration
MTT	3-[4,5-dimethylthiazol-2-yl]-2,5-diphenyl-2H-tetrazolium bromide
<i>P. aeruginosa</i>	<i>Pseudomonas aeruginosa</i>
<i>P. vulgaris</i>	<i>Proteus vulgaris</i>
PBS	phosphate buffer saline
<i>S. aureus</i> (MRSA)	<i>Staphylococcus aureus</i> (Methicillin-resistant <i>Staphylococcus aureus</i>)
<i>S. enterica</i>	<i>Salmonella enterica</i>
<i>S. epidermidis</i>	<i>Staphylococcus epidermidis</i>

<i>S. flexneri</i>	<i>Shigella flexneri</i>
<i>S. saprophyticus</i>	<i>Staphylococcus saprophyticus</i>
<i>S. maltophilia</i>	<i>Stenotrophomonas maltophilia</i>

Appendix A. Supplementary data

CCDC 1920543 and 1920546 contains the supplementary crystallographic data for **1** and **3**. These data can be obtained free of charge via <http://www.ccdc.cam.ac.uk/conts/retrieving.html>, or from the Cambridge Crystallographic Data Centre, 12 Union Road, Cambridge CB2 1EZ, UK; fax: (+44) 1223-336-033; or e-mail: deposit@ccdc.cam.ac.uk

^1H and $^{13}\text{C}\{^1\text{H}\}$ NMR data, thermal decomposition data and CC_{50} data are given in Tables SI1-SI4 while ^1H and $^{13}\text{C}\{^1\text{H}\}$ NMR spectra, representative traces and crystallographic diagrams (including geometric data characterising the intermolecular contacts) are given in and Figures SI1-SI20. Supplementary data to this article can be found online at <https://doi.org/10.1016/j.poly.2022.xxxxxx>.

References

- [1] A.G. Davies, *Organotin Chemistry* (2nd Edition), Wiley-VCH, Weinheim, Germany, 2004.
- [2] A.G. Davies, M. Gielen, K.H. Pannell, E.R.T. Tiekink eds., *Tin Chemistry: Fundamentals, Frontiers and Applications*, Wiley, UK, 2008.
- [3] S.K. Hadjikakou, N. Hadjiliadis, *Coord. Chem. Rev.* 253 (2009) 235-249.
<https://doi.org/10.1016/j.ccr.2007.12.026>.
- [4] T. Anasamy, C.F. Chee, Y.F. Wong, C.H. Heh, L.V. Kiew, H.B. Lee, L.Y. Chung, *Appl. Organomet. Chem.* 35 (2021) e6089. <https://doi.org/10.1002/aoc.6089>.
- [5] C.E. Carraher, M.R. Roner, *J. Organomet. Chem.* 751 (2014) 67-82.
<https://doi.org/10.1016/j.jorganchem.2013.05.033>.
- [6] S E.H. Etaiw, T.A. Fayed, M.M. El-bendary, H. Marie, *Appl. Organometal Chem.* 32 (2018) e4066. <https://doi.org/10.1002/aoc.4066>.
- [7] S.E.H. Etaiw, M.M. El-bendary, *Polyhedron* 87 (2015) 383-389.
<https://doi.org/10.1016/j.poly.2014.12.011>.
- [8] S. Tabassum, C. Pettinari, *J. Organomet. Chem.* 691 (2006) 1761-1766.
<https://doi.org/10.1016/j.jorganchem.2005.12.033>.
- [9] B. Gleeson, J. Claffey, D. Ertler, M. Hogan, H. Müller-Bunz, F. Paradisi, D. Wallis, M. Tacke, *Polyhedron* 27 (2008) 3619-3624. <https://doi.org/10.1016/j.poly.2008.09.009>.
- [10] M. Nath, P.K. Saini, *Dalton Trans.* 40 (2011) 7077-7121.
<https://doi.org/10.1039/C0DT01426E>.
- [11] J. Devi, S. Devi, J. Yadav, A. Kumar, *ChemistrySelect* 4 (2019) 4512-4520.
<https://doi.org/10.1002/slct.201900317>.
- [12] K.T. Mahmudov, M.F.C G. Da Silva, M.N. Kopylovich, A.R. Fernades, A. Silva, A. Mizar, A.J.L. Pombeiro, *J. Organometal. Chem.* 760 (2014) 67-73.
<https://doi.org/10.1016/j.jorganchem.2013.12.019>.

- [13] A. Kapila, M. Kaur, H. Kaur, *Mater. Today: Proc*, 40 (2021) S102-S106. <https://doi.org/10.1016/j.matpr.2020.04.080>.
- [14] J. Devi, S. Pachwania, D. Kumar, D.K. Jinal, S. Jan, A.K. Dash, *Res. Chem. Intermed.* 48 (2022) 267–289. <https://doi.org/10.1007/s11164-021-04557-w>.
- [15] R. Vinayak, D. Dey, D. Ghosh, D. Chattopadhyay, A. Ghosh, H.P. Nayek, *Appl Organometal Chem.* 32 (2018) e4122. <https://doi.org/10.1002/aoc.4122>.
- [16] K. Liu, H. Yan, G. Chang, Z. Li, M. Niu, M. Hong, *Inorg. Chim. Acta* 464 (2017) 137-146. <https://doi.org/10.1016/j.ica.2017.05.017>.
- [17] M. Hong, H. Yin, X. Zhang, C. Li, C. Yue, S. Cheng, *J. Organomet. Chem.* 724 (2013) 23-31. <https://doi.org/10.1016/j.jorganchem.2012.10.031>.
- [18] W. Rehman, A. Badshah, S. Khan, L.T.A. Tuyet, *Eur. J. Med. Chem.* 44 (2009) 3981-3985. <https://doi.org/10.1016/j.ejmech.2009.04.027>.
- [19] T.S. Basu Baul, *Appl. Organomet. Chem.* 22 (2008) 195-204. <https://doi.org/10.1002/aoc.1378>.
- [20] J. Devi, J. Yadav, N. Singh, *Res. Chem. Intermed.* 45 (2019) 3943–3968. <https://doi.org/10.1007/s11164-019-03830-3>.
- [21] T. Sedaghat, Y. Ebrahimi, L. Carlucci, D. M. Proserpio, V. Nobakht, H. Motamedi, M.R. Dayer, *J. Organomet. Chem.* 794 (2015) 223-230. <https://doi.org/10.1016/j.jorganchem.2015.06.034>.
- [22] L.C. Dias, G.M. de Lima, J.A. Takahashi, J.D. Ardisson, *Appl. Organomet. Chem.* 29 (2015) 305-313. <https://doi.org/10.1002/aoc.3292>.
- [23] S. Shujah, Z. Rehman, N. Muhammad, S. Ali, N. Khalid, M.N. Tahir, *J. Organomet. Chem.* 696 (2011) 2772-2781. <https://doi.org/10.1016/j.jorganchem.2011.04.010>.
- [24] S. Shujah, Z. Rehman, N. Muhammad, A. Shah, S. Ali, A. Meetsma, Z. Hussain, *J. Organomet. Chem.* 759 (2014) 19-26. <https://doi.org/10.1016/j.jorganchem.2014.02.010>.

- [25] A. González, E. Gómez, A. Cortés-Lozada, S. Hernández, T. Ramírez-Apan, A. Nieto-Camacho, *Chem. Pharm. Bull.* 57 (2009) 5-15. <https://doi.org/10.1248/cpb.57.5>.
- [26] M. Nath, P.K. Saini, A. Kumar, *J. Organometal. Chem.* 695 (2010) 1353-1362. <https://doi.org/10.1016/j.jorganchem.2010.02.009>.
- [27] E.R.T. Tiekink, *Appl. Organomet. Chem.* 22 (2008) 533-550. <https://doi.org/10.1002/aoc.1441>.
- [28] N. Rabiee, M. Safarkhani, Moein, M.M. Amini, *Rev. Inorg. Chem.* 39 (2019) 13-45. <https://doi.org/10.1515/revic-2018-0014>.
- [29] N. Khan, Y. Farina, L.K. Mun, N.F. Rajab, N. Awang, *Polyhedron* 85 (2015) 754-760. <https://doi.org/10.1016/j.poly.2014.08.063>.
- [30] T.S. Basu Baul, R. Manne, A. Duthie, L.Y. Liew, J. Chew, S.M. Lee, E.R.T. Tiekink. *J. Organomet. Chem.* 941 (2021) 121802. <https://doi.org/10.1016/j.jorganchem.2021.121802>.
- [31] Y.-X. Tan, Z.-J. Zhang, Y. Liu, J.-X. Yu, X.-M. Zhu, D.-Z. Kuang, W.-J. Jiang, *J. Mol. Struct.* 1149 (2017) 874-881. <https://doi.org/10.1016/j.molstruc.2017.08.058>.
- [32] S. Hussain, S. Ali, S. Shahzadi, M.N. Tahir, M. Shahid, K.S. Munawar, S.M. Abbas, *Polyhedron* 117 (2016) 64-72. <https://doi.org/10.1016/j.poly.2016.05.045>.
- [33] M. Hong, H.-D. Yin, S.-W. Chen, D.-Q. Wang, *J. Organomet. Chem.* 605 (2010) 653-662. <https://doi.org/10.1016/j.jorganchem.2009.11.035>.
- [34] E.N.M. Yusof, A.J. Page, J.A. Sakoff, M.I. Simone, A. Veerakumarasivam, E.R.T. Tiekink, T.B.S.A. Ravoof, *Polyhedron* 189 (2020) 114729. <https://doi.org/10.1016/j.poly.2020.114729>.
- [35] H.N. Dogan, S. Rollas, H. Erdeniz, *Il Farmaco* 53 (1998) 462-467. [https://doi.org/10.1016/S0014-827X\(98\)00049-4](https://doi.org/10.1016/S0014-827X(98)00049-4).
- [36] S.M. Lee, K.S. Sim, K.M. Lo, *Inorg. Chim. Acta* 429 (2015) 195-208. <https://doi.org/10.1016/j.ica.2015.01.017>.

- [37] S.M. Lee, H.M. Ali, K.S. Sim, S.R.A. Malek, K.M. Lo, *Appl. Organomet. Chem.* 26 (2012) 310-319. <https://doi.org/10.1002/aoc.2862>.
- [38] S.M. Lee, H. M. Ali, K. S. Sim, S.R.A. Malek, K.M. Lo, *Inorg. Chim. Acta* 406 (2013) 272-278. <https://doi.org/10.1016/j.ica.2013.04.036>.
- [39] K. Sisido, Y. Takeda, Z. Kinugawa, *J. Am. Chem. Soc.* 83 (1961) 538-541. <https://doi.org/10.1021/ja01464a008>.
- [40] W.L.F. Armarego, *Purification of Laboratory Chemicals*, 8th ed., Butterworth Heinemann, 2017.
- [41] CrysAlis PRO, Agilent Technologies, Yarnton, England, 2012.
- [42] CrysAlis PRO, Rigaku Oxford Diffraction, Yarnton, Oxfordshire, England, 2017.
- [43] G.M. Sheldrick, *Acta Crystallogr* A64 (2008) 112-122. <https://doi.org/10.1107/S0108767307043930>.
- [44] G.M. Sheldrick, *Acta Crystallogr.* C71 (2015) 3-8. <https://doi.org/10.1107/S2053229614024218>.
- [45] L.J. Farrugia, *J. Appl. Crystallogr.* 45 (2012) 849-854. <https://doi.org/10.1107/S0021889812029111>.
- [46] K. Brandenburg, DIAMOND. Visual Crystal Structure Information System, version 3.1, Crystal Impact, Bonn, Germany, 2006.
- [47] A.L. Spek, *Acta Crystallogr* E76 (2020) 1-11. <https://doi.org/10.1107/S2056989019016244>.
- [48] C.H. Tan, D.S.Y. Sim, M.P. Heng, S.H. Lim, Y.Y. Low, T.S. Kam, K.S. Sim, *Chemistry Select* 5 (2020) 14839-14843. <https://doi.org/10.1002/slct.202004153>.
- [49] S. Desai, V. Desai, S. Shingade, *Bioorganic Chem.* 94 (2020) 103382. <https://doi.org/10.1016/j.bioorg.2019.103382>.

- [50] H. Yin, S.W. Chen, *Inorg. Chim. Acta* 359 (2006) 3330-3338.
<https://doi.org/10.1016/j.ica.2006.03.024>.
- [51] H. D. Yin, M. Hong, G. Li, D. Q. Wang, *J. Organomet. Chem.* 690 (2005) 3714-3719.
<https://doi.org/10.1016/j.jorganchem.2005.04.049>.
- [52] H. D. Yin, S. W. Chen, L. W. Li, D. Q. Wang, *Inorg. Chim. Acta* 360 (2007) 2215-2223.
<https://doi.org/10.1016/j.ica.2006.10.038>.
- [53] M. A. Salam, R. A. Haque, *Inorg. Chim. Acta* 435 (2015) 103-108.
<https://doi.org/10.1016/j.ica.2015.06.015>.
- [54] T. S. Basu Baul, W. Rynjah, X. Song, G. Eng, A. Linden, *J. Organometal. Chem.* 692 (2007) 3392-3399. <https://doi.org/10.1016/j.jorganchem.2007.04.002>.
- [55] H.D. Yin, M. Hong, G. Li, D.Q. Wang, *J. Organomet. Chem.* 690 (2005) 3714-3719.
<https://doi.org/10.1016/j.jorganchem.2005.04.049>.
- [56] H.D. Yin, M. Hong, Q.B. Wang, S.C. Xue, D. Q. Wang, *J. Organomet. Chem.* 690 (2005) 1669-1676. <https://doi.org/10.1016/j.jorganchem.2004.12.037>.
- [57] M. Hanif, M. Hussain, S. Ali, M H. Bhatti, M.S. Ahmed, B. Mirza, H. Stoeckli-Evans, *Polyhedron* 29 (2010) 613-619. <https://doi.org/10.1016/j.poly.2009.07.039>.
- [58] C. González-García, A. Mata, F. Zani, M.A. Mendiola, E. López-Torres, *J. Inorg. Biochem.* 163 (2016) 118-130. <https://doi.org/10.1016/j.jinorgbio.2016.07.002>.
- [59] T.S. Basu Baul, M.R. Addepalli, A. Lyčka, S. van Terwingen, U. Engler, *J. Organomet. Chem.* 927 (2020) 121522. <https://doi.org/10.1016/j.jorganchem.2020.121522>.
- [60] T.P. Lockhart, W.F. Manders, *Inorg. Chem.* 25 (1986) 892-895.
<https://doi.org/10.1021/ic00227a002>.
- [61] T. P. Lockhart, W.F. Manders, J. J. Zuckerman, *J. Am. Chem. Soc.* 107 (1985) 4546-4547.
<https://doi.org/10.1021/ja00301a030>.

- [62] M. Nádvorník, J. Holeček, K. Handlíř, A. Lyčka, *J. Organomet. Chem.* 275 (1984) 43-51.
[https://doi.org/10.1016/0022-328X\(84\)80576-8](https://doi.org/10.1016/0022-328X(84)80576-8).
- [63] A. Lyčka, J. Holeček, M. Nádvorník, K. Handlíř, *J. Organomet. Chem.* 280 (1985) 323-329. [https://doi.org/10.1016/0022-328X\(85\)88109-2](https://doi.org/10.1016/0022-328X(85)88109-2).
- [64] J. Holeček, M. Nádvorník, K. Handlíř, A. Lyčka, *J. Organomet. Chem.* 315 (1986) 299-308. [https://doi.org/10.1016/0022-328X\(86\)80450-8](https://doi.org/10.1016/0022-328X(86)80450-8).
- [65] U. Sair, A. Thakur, *Mater Today-Proc.* 50 (2022) 1862-1866,
<https://doi.org/10.1016/j.matpr.2020.04.080>.
- [66] S. Yaqub, F. Ahmed, S. Rehman, S. Shahzadi, *J. Iran. Chem. Soc.* 6 (2009) 88-98.
<https://doi.org/10.1007/bf03246506>
- [67] R. Singh, N. K. Khausik, *Spectrochim. Acta, Part A* 71 (2008) 669-675.
<https://doi.org/10.1016/j.saa.2008.01.015>.
- [68] A.W. Addison, T.N. Rao, J. Reedijk, J. van Rijn, C.C. Verschoor, *J. Chem. Soc. Daltons Trans.* (1984) 1349-1356. <https://doi.org/10.1039/DT9840001349>.
- [69] I. J. Bruno, J. C. Cole, P. R. Edgington, M. Kessler, C. F. Macrae, P. McCabe, J. Pearson and R. Taylor, *Acta Crystallogr.* B58 (2002) 389-397.
- [70] S.M. Lee, K.M. Lo, H.M. Ali, S.W. Ng, *Acta Crystallogr.* E65 (2009) m816
10.1107/S1600536809022259.
- [71] S.M. Lee, H.M. Ali, K.M. Lo, *Acta Crystallogr.* E66 (2010) m161
10.1107/S1600536810001133.
- [72] S.N.B.M. Rosely, R.S.D. Hussen, S.M. Lee, N.R. Halcovitch, M.M. Jotani, E.R.T. Tiekink, *Acta Crystallogr.* E73 (2017) 390 10.1107/S2056989017002365
- [73] S.M. Lee, K.M. Lo, H.M. Ali, S.W. Ng, *Acta Crystallogr.* E65 (2009) m862
10.1107/S1600536809024477

- [74] S.M. Lee, K.M. Lo, H.M. Ali, S.W. Ng, *Acta Crystallogr. E* 65 (2009) m1689
10.1107/S1600536809050107
- [75] S.M. Lee, H.M. Ali, K.M. Lo *Acta Crystallogr. E* 66 (2010) m162
10.1107/S1600536810001145
- [76] D. Ahmed, P. W. Eide, I. A. Eilertsen, S. A. Danielsen, M. Eknæs, M. Hektoen, G. E. Lind, R. A. Lothe, *Oncogenesis* 2 (2013) e71. <https://doi.org/10.1038/oncsis.2013.35>.
- [77] E. Tacconelli, E. Carrara, A. Savoldi, S. Harbarth, M. Mendelson, D. L. Monnet, C. Pulcini, G. Kahlmeter, J. Kluytmans, Y. Carmeli, *Lancet Infect. Dis.* 18 (2018) 318-327.
[https://doi.org/10.1016/S1473-3099\(17\)30753-3](https://doi.org/10.1016/S1473-3099(17)30753-3).